IOPscience iopscience.iop.org

Home Search Collections Journals About Contact us My IOPscience

Charge order in the extended Hubbard model

This article has been downloaded from IOPscience. Please scroll down to see the full text article.

2003 J. Phys.: Condens. Matter 15 8363

(http://iopscience.iop.org/0953-8984/15/49/014)

View the table of contents for this issue, or go to the journal homepage for more

Download details:
IP Address: 171.66.16.125
The article was downloaded on 19/05/2010 at 17:51

Please note that terms and conditions apply.

INSTITUTE OF PHYSICS PUBLISHING JOURNAL OF PHYSICS: CONDENSED MATTER

J. Phys.: Condens. Matter **15** (2003) 8363–8375 PII: S0953-8984(03)65266-5

Charge order in the extended Hubbard model

Krzysztof Rościszewski and Andrzej M Oleś

M Smoluchowski Institute of Physics, Jagellonian University, Reymonta 4, PL-30059 Kraków, Poland

Received 23 June 2003
Published 25 November 2003
Online at stacks.iop.org/JPhysCM/15/8363

Abstract

Magnetic and charge order in half-filled and doped finite two-dimensional (8×8) clusters described by the extended Hubbard Hamiltonian with medium to large on-site (U) and intersite (V) Coulomb repulsion were investigated using correlated wavefunctions. The treatment of spatially inhomogeneous correlations was possible thanks to a combination of the local ansatz and the local increments expansion methods. The surprising result is that in the half-filled case the correlations do not influence the transition from the antiferromagnetic (AF) to charge order (CO) phase found in the Hartree–Fock approximation. For the doped systems we found a variety of stripe or superlattice-like structures for small values of V, while for larger V we identified robust CO phases. For smaller doping ($\delta = 1/8$ and $1/4$) the charge-majority sublattice has typically inhomogeneous charge distribution and is decorated by various magnetic patterns, while for larger doping ($\delta = 1/2$) the co-phase is homogeneous (ideal) and with superimposed AF order.

1. Inhomogeneous spin and charge order in transition metal oxides

Inhomogeneous charge and spin ordering in real space, so-called stripe phases, have attracted much attention due to their possible role in the high temperature superconductivity of the cuprates. They were first predicted in the Hartree–Fock (HF) [1] calculations and later observed in x-ray and in neutron scattering experiments for $La_{2-x}Sr_xCuO_4$ and $YBa_2Cu_3O_{6+x}$ [2], as well as in nickelate systems [3]. They are generally described in terms of a two-dimensional (2D) Hubbard (or three-band) model with intermediate to strong on-site repulsion U [4]. A possible role of the nearest neighbour Coulomb repulsion V on the stripe stability was also investigated [5] for the systems with relatively small doping $\delta = 1 - n$ (typically $1/8$), where n is the band filling.

For systems with larger hole concentrations, however, not the stripe phases, but the phases with charge order (CO) were reported instead (Yb_4As_3 [6], NaV_2O_5 [7], in colossal magnetoresistance compounds at $\delta = 1/2$ doping like in cubic $RE_{1/2}(Sr, Ca)_{1/2}MnO_3$ [8], bilayer $LaSr_2Mn_2O_7$ [9] and single-layer $La_{1/2}Sr_{1/2}MnO_4$ [10] manganites, and also in

 © 2003 IOP Publishing Ltd Printed in the UK

nickelates $La_{1.5}Sr_{0.5}NiO_4$ [11]). The theoretical investigations of the CO in 2D and three-dimensional (3D) systems with Coulomb intersite and intrasite repulsion are numerous and include Green function methods [12], local ansatz [13], numerical Monte Carlo simulation [14], the HF approximation [15], $1/d$ perturbation expansion around the infinite-dimensional ($d = \infty$) hypercubic lattice solution [16], the dynamical mean-field theory [17], numerical Lanczos technique [18], variants of mean-field approach [19], and lastly coherent potential approximation [20].

All of these approaches yield useful results but as a rule strong simplifying assumptions about the ground state symmetry must be made as a starting point. This is well justified for the cases when the ground state symmetry is a simple one, but in general the problem of inhomogeneous charge and spin ordering remains difficult and is still open. Motivated by the above experiments, we address this problem in the present work by correlation computations of inhomogeneous spin and charge distribution in the extended Hubbard model.

The paper is organized as follows. We present the model and discuss the variational method in section 2. The local increments (LI) expansion of the correlation energy is explained in section 3. In section 4 we present detailed numerical results obtained for various model parameters and doping levels, while more general concluding remarks are presented in section 5.

2. The model and the variational method

We study the extended single-band Hubbard Hamiltonian (at temperature $T = 0$),

$$H = \sum_{ij\sigma} t_{ij} c^{\dagger}_{i\sigma} c_{j\sigma} + U \sum_{i} n_{i\uparrow} n_{i\downarrow} + V \sum_{\langle i,j \rangle} n_i n_j. \tag{1}$$

Here $c^{\dagger}_{i\sigma}$ ($c_{i\sigma}$) are creation (annihilation) operators for an electron with spin $\sigma = \uparrow, \downarrow$ at site i, and $n_{i\sigma} = c^{\dagger}_{i\sigma} c_{i\sigma}$ are electron number operators. The hopping elements are finite, $t_{ij} = -t$, on the bonds $\langle i, j \rangle$ which connect nearest neighbours and zero otherwise. The sum $\langle i, j \rangle$ runs over all nearest neighbour pairs. The on-site repulsion U was taken to be 4, 6, 8 and 10 (in units of hopping element t)—typical weak to strong correlation values. The intersite repulsion V was varied from 0 up to $U/2$. The attractive U and/or V interactions were not studied.

We considered 2D square clusters containing $N = 64$ sites with periodic boundary conditions, i.e., an 8×8 supercell, at half-filling ($n = 1$, where n is an average electron density), and with hole doping $\delta = 1 - n = 1/8, 1/4, 1/2$. First, the calculations within the HF approximation were performed to determine the ground state wavefunction $|\Psi_{\rm HF}\rangle$ and HF ground state energy $E_{\rm HF} = \langle \Psi_{\rm HF}|H|\Psi_{\rm HF}\rangle$.

In the next step the HF wavefunction was modified to include the electron correlation effects. We used an exponential ansatz [21] for the correlated ground state,

$$|\Psi\rangle = \exp\left(-\sum_{\mu} \alpha_{\mu} O_{\mu}\right)|\Psi_{\rm HF}\rangle, \tag{2}$$

where O_{μ} are the local operators selected to perform the correlation calculations, and α_{μ} are the corresponding variational parameters. In this way, the ground state wavefunction $|\Psi\rangle$ can be optimized and energetically unfavourable configurations, such as double occupancies at one site and large charge fluctuations, are suppressed.

The first type of the O_{μ} operators we used is $\delta n_{i\uparrow}\delta n_{i\downarrow}$, where $\delta n_{i\uparrow}$ indicates taking that part of the $n_{i\uparrow}$ operator which annihilates one occupied single particle HF state and creates an electron in one of the virtual states. When acting on the HF wavefunction the operator $\delta n_{i\uparrow}\delta n_{i\downarrow}$ is equivalent to $n_{i\uparrow}n_{i\downarrow} - \langle n_{i\uparrow}n_{i\downarrow}\rangle$, introduced in the framework of the local ansatz

method a long time ago [21]. (The explicit expression for any operator is lengthy and can be provided only after using the transformation from the real space $\{c^{\dagger}_{i\sigma}\}$ operators to creation operators corresponding to single-particle HF eigenstates.) As usual, the average $\langle\cdots\rangle$ stands for the average over the HF ground state.

The second and the third types of the local operators optimize the intersite charge correlations for equal and different spin; we used $\delta n_{i\uparrow}\delta n_{j\downarrow}+\delta n_{j\uparrow}\delta n_{i\downarrow}$ and $\delta n_{i\uparrow}\delta n_{j\uparrow}+\delta n_{i\downarrow}\delta n_{j\downarrow}$, with i and j being nearest neighbours, next (second) nearest neighbours and the third nearest neighbours. Again, these are close counterparts of commonly used local charge and spin operators [21] (but they are not identical).

The variational parameters $\{\alpha_\mu\}$ were fixed by minimizing the total energy E in the correlated ground state $|\Psi\rangle$:

$$E = \frac{\langle\Psi|H|\Psi\rangle}{\langle\Psi|\Psi\rangle}. \tag{3}$$

If electron correlations are not too strong, the total energy E can be evaluated by using expansion of the wavefunction equation (2) up to second-order terms $\propto\alpha_\mu\alpha_\nu$. To obtain the formula for the ground state energy E one needs to compute numerous (and computationally quite costly) averages of the type $a_{\mu\nu} = \langle O_\mu(H - E_{\rm HF})O_\nu\rangle$ and $b_\mu = \langle O_\mu H\rangle$. The correlation energy $E_{\rm corr} = E - E_{\rm HF}$ may be written in terms of $\boldsymbol{a}$ matrix and $\boldsymbol{b}$ vector as follows: $E_{\rm corr} = -\boldsymbol{b}^{\rm T}\boldsymbol{a}^{-1}\boldsymbol{b}$ [21].

We computed $\langle O_\mu(H - E_{\rm HF})O_\nu\rangle$ not exactly, but by using the HF part of H; this may be considered a 'leading-order' approximation [22]. Unfortunately, even within this approximation the correlation treatment for nonhomogenous systems is a difficult task. In our 8×8 cluster one has to determine 320 different coefficients $\{\alpha_\mu\}$. It turns out that the matrix $\langle O_\mu(H - E_{\rm HF})O_\nu\rangle$ is frequently ill conditioned and/or oversensitive to numerical rounding errors which, together with the bulk of computations (one has to perform), forces one to use another method which does not attempt to get all the coefficients $\{\alpha_\mu\}$ at once (in a single step), but rather such a method that the number of α_μ in each individual computational step is small. Therefore, we used LI expansion [23], the method which was introduced by Stoll in 1992 and which made the correlation treatment of solids (and large clusters) reasonably 'inexpensive' since then [24].

3. Local increments expansion

The LI expansion for the total correlation energy in our case is defined as [23]

$$E_{\rm corr} = S_1 + S_2 + \cdots = \sum_I \Delta\varepsilon_I + \sum_{I<J} \Delta\varepsilon_{IJ} + \cdots, \tag{4}$$

where $I, J, K, \ldots$ denote the groups of occupied localized orbitals placed everywhere in the crystal. The quantity $\Delta\varepsilon_I$ (a one-body increment) coincides by definition with the correlation energy $\varepsilon(I)$ contribution due to local correlations at the Ith site only, i.e., $\Delta\varepsilon_I \equiv \varepsilon(I)$. Note that all orbitals other than I are frozen. The method to compute $\varepsilon(I)$ depends on a particular implementation and is irrelevant for the LI expansion (here we use the local ansatz [21]).

The two-body increment $\Delta\varepsilon_{IJ}$ is defined as the non-additive (irreducible) part of the intersite correlation energy resulting from correlating the orbitals at sites I and J simultaneously:

$$\Delta\varepsilon_{IJ} = \varepsilon(IJ) - \Delta\varepsilon_I - \Delta\varepsilon_J, \tag{5}$$

where $\varepsilon(IJ)$ is total correlation energy of the crystal in which both I and J sites are correlated (at the same time). Similarly, one can define three-body increments, etc.

Table 1. The HF energy $(E_{\mathrm{HF}}/N)-2V$, and the energy with correlation contributions $(E/N)-2V$ per atom (in units of hopping element t), as obtained for different AF or CO phases in a 2D cluster for $U = 8$ and $n = 1$ (for convenience, the average on-site potential energy $2V$, as obtained in the HF approximation, was subtracted). The one-body S_1/N and two-body S_2/N correlation increments (per atom) are also given.

V	$(E_{\mathrm{HF}}/N)-2V$	$(E/N)-2V$	S_1/N	S_2/N	Phase
0.0	−0.4658	−0.4779	−0.014 27	0.002 17	AF
1.0	−0.5175	−0.5301	−0.013 20	0.000 56	AF
2.0	−0.5783	−0.5958	−0.011 07	−0.006 44	AF
2.0	−0.5783	−0.5958	−0.011 07	−0.006 44	CO
2.5	−0.6124	−0.6355	−0.009 61	−0.013 45	AF
2.5	−1.3955	−1.3989	−0.001 39	−0.001 94	CO

The expansion given by equation (4) if carried out up to infinity is exact. For practical applications, however, one has to truncate the infinite series. Numerous papers on the LI expansion applied in different systems [24] gave convincing evidence that the LI expansion is in general quickly convergent and that the three-body and four-body increments are small and in most cases negligible. Moreover, the two-body increments equation (5) rapidly decays for larger distances (i.e., when I and J are located far apart) greatly saving on computational efforts [24].

Therefore, we take first- and second-order increments only, the second-order increments being calculated for nearest neighbours up to the third order. Typical examples of the data obtained by this approach are shown in table 1.

4. Numerical results

First we performed HF computations starting from several different initial charge and spin configurations. The minimized energy E_{HF} has (in many cases) a multitude of local minima. In this respect too few HF starting configurations might result in a failure to find the true ground state within this method, and instead some local minimum would mimic the ground state (within a restricted class of solutions). Therefore, a tremendous effort is needed when one wants to be reasonably sure that the global minimum found is the correct one. For the sake of present study, for each set of U and V we picked 50 different and carefully chosen starting configurations. We wanted account for any (possible in principle) ground state known from the literature, such as antiferromagnetic (AF) order, various stripe phases, polaronic-like configurations and various CO phases with inhomogeneous charge and magnetization density distribution.

As a result of the numerical procedure described we obtained numerous HF-stable (i.e., converged within the HF method) phases with different energy and/or different spin and charge patterns. For each such phase we performed LI correlation computations obtaining the final (total) energy, $E = E_{\mathrm{HF}} + E_{\mathrm{corr}}$. The minimal value of E extracted from the set of up to 50 individual values of E served to identify the true ground state (frequently the number of self-consistent solutions is lower than 50 as not necessarily all HF runs starting from different initial configurations turn out to be convergent). Alongside this computational effort we paid much attention to achieving good HF convergence; therefore, not only the HF energy but also on-site densities and several rather sensitive correlation functions were required to converge simultaneously.

4.1. Half-filled (undoped) case

The possibility of the CO phase in the extended Hubbard model was investigated in the pioneering work by Robaszkiewicz about three decades ago [12]. The technique employed

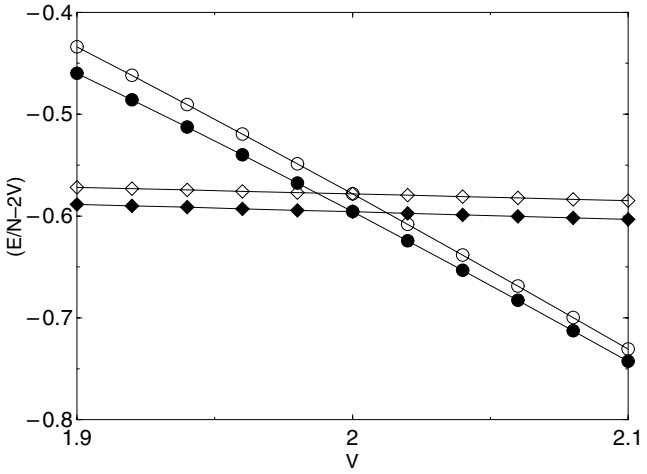

Figure 1. The energies per site of the AF (diamonds) and CO (circles) phase as functions of V in the HF approximation (open symbols), and using the correlation corrections (filled symbols), for the half-filled case ($n = 1$) at $U = 8$; all energies are in units of the hopping element t. The transition from the AF to CO phase occurs at $V = 2$ (see also table 1).

at that time was the temperature Green function method (very similar to that employed by Hoang and Thalmeier recently [20]) with strong simplifying assumptions. As in the present investigation we are interested only in $T = 0$ ground state solutions, and as we want to include correlations as precisely as possible (in an *ab initio* manner), we numerically investigated the CO in finite clusters as explained in the previous section. For the half-filled case (simple square 2D lattice) we found a transition from the AF to CO phase at $zV = U$ (see figure 1), where $z = 4$ is the lattice coordination number. The CO phase is nonmagnetic and consists of two space-homogeneous sublattices: the charge-majority one and charge-minority one (arranged like the black and white fields on a chessboard). For some computational details see table 1.

The surprising result is that the correlations do not influence the transition between the AF and CO phases, i.e., the critical HF value of $zV = U$ remains the same also in the presence of electron correlations (see figure 1). The test computations performed for periodic $4 \times 4 \times 4$ clusters confirmed that the critical value connected with the transition from the AF to CO phase is also $zV = U$ for a 3D system (here $z = 6$ is the coordination number for a 3D simple cubic lattice). Let us mention that a clear indication (in the form of analytic inequalities) suggesting such a behaviour was published about two decades ago [13].

4.2. Charge order for weak interaction $U = 4$ and increasing doping

For small values of intersite Coulomb potential V the most stable phases at doping $\delta = 1/8$ are weakly inhomogeneous spin and charge patterns, with lines of nonmagnetic atoms in between the AF domains oriented in a diagonal (11) (or $(1\bar{1})$) direction, and separated by four lattice constants along the $x(y)$ direction from each other. The diagonal orientation is sometimes intermingled with vertical order. Such structures are usually called *stripe phases* (not shown). A typical pattern consists of repeating nonmagnetic diagonal domain walls, one line thick, which separate the AF domains which contain three lines of magnetic atoms each.

The first indication of relatively weak CO starts to appear for $V \simeq 0.5$. CO reflects the lattice symmetry in the simplest way, i.e., the charges (on average) are self-organized according to a cubic bipartite lattice principle (with charge-majority and charge-minority sublattices). A spin order coexists with CO in a broad parameter regime, but first (for $0.5 < V < 1.0$) only

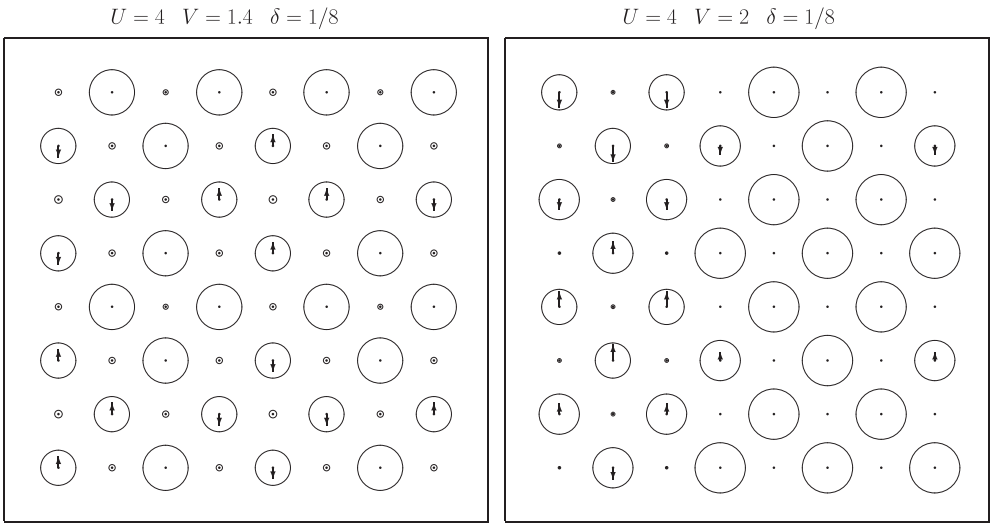

Figure 2. Magnetic and charge order as obtained for an 8×8 cluster with $U = 4$ for doping $\delta = 1/8$, and for $V = 1.4$ (left) and $V = 2.0$ (right). The circle diameters correspond to the on-site charges, and the arrow lengths to the spin values expressed in the natural scale (i.e., measured in nearest-neighbour atom–atom distance which is taken to be unity)[1].

isolated polarons occur, while at larger values of V they form four-atom clusters, and finally the system separates into the phase with lower (average) charge density and magnetic moments, and a CO phase with higher average density. The typical examples of the latter phases are shown in figure 2. While at $V \simeq 1.4$ the CO state consists of four-site islands of magnetic atoms separated by the nonmagnetic atoms with higher electron density, at higher values of $V \simeq 2.0$ this pattern is unstable and one finds a phase separation into a magnetic phase, with two ferromagnetic (FM) domains, and the CO nonmagnetic phase. In both phases the electron density is high only at one sublattice A, while at the sublattice B it is close to zero.

At higher doping ($\delta = 1/4$) the stripe phases are unstable and one finds instead a uniform nonmagnetic phase with homogeneous charge distribution in the entire range of $0 < V < 1.3$, while starting from $V = 1.4$ the CO is more stable and persists up to $V = 2.0$. The charge majority sublattice, with the electron filling $n > 1$ per site, shows weak charge modulation. At the same time magnetic moments occur at the atoms with larger charge density, and are on average ferromagnetically arranged in vertical domains (figure 3). In our 8×8 cluster we found two FM domains with opposite magnetization. The charge-minority sublattice is nonmagnetic in all cases.

For the case of quarter filling ($n = 1/2$) the charge is usually ordered in a symmetric way. At small V neither typical stripe phases are stable, nor CO phases. Instead, a superlattice-type spin ordering takes over (compare with a similar behaviour found for $U = 6$ and $\delta = 1/2$, reported below). Starting from $V = 1.5$, CO and magnetic inhomogeneities start to appear—some of them resemble polaronic behaviour. For $V = 2.0$ a CO phase with the ideal bipartite pattern sets in (figure 3). The majority-charge sublattice is AF, while the minority one is nonmagnetic and almost empty. We call the CO phase displayed in the right-hand panel of figure 3 an *ideal CO phase*.

[1] The proportionality of circle diameters and arrow lengths to the true charges and spins is quite poor. The figures were prepared using LaTex 'circle' (or 'vector') commands. Only certain sizes of the circles are available, so LaTex selects the one closest to the specified diameter entry. Compare for example [25].

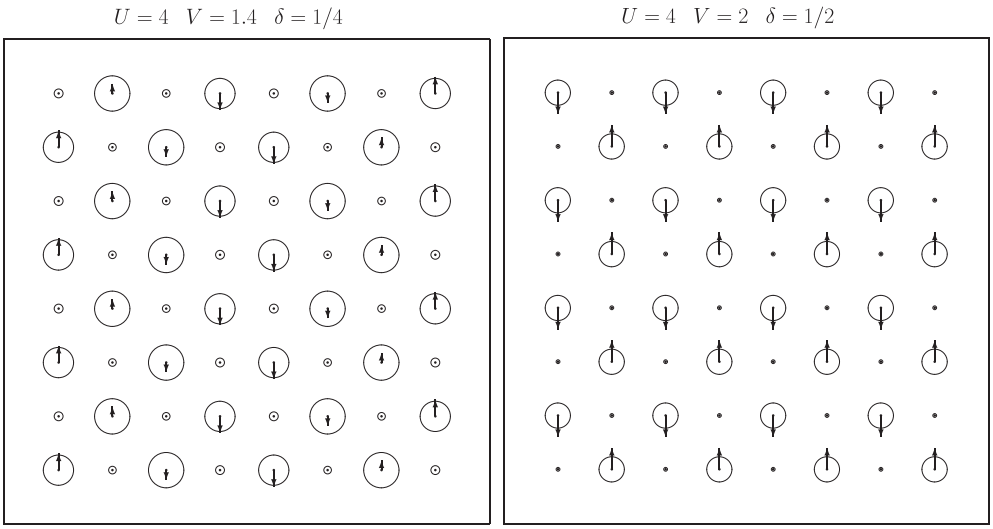

Figure 3. Magnetic and charge order as obtained for an 8×8 cluster with $U = 4$ for two different values of doping: left—$\delta = 1/4$ at $V = 1.4$, and right—$\delta = 1/2$ at $V = 2.0$. The meaning of circles and arrows is the same as in figure 2.

4.3. Charge order in the intermediate interaction regime, $U = 6$

First, we consider again the low doping regime $\delta = 1/8$. In the interval between $V = 0.0$ and $V = 1.4$ we identified several stripe phases. The orientation patterns are diagonal (at $V \simeq 0$) and vertical (at $V > 0.2$); a typical example is shown in the left-hand panel of figure 4. Interestingly, the lines of atoms with the lowest electron density are weakly *ferromagnetic*, in contrast to the vertical stripe phase with *nonmagnetic* on-site domain walls, found before in the calculations beyond the HF approximation [22, 26]. We note that the present novel stripe phase represents an intermediate situation between the on-site domain walls [1] and the on-bond domain walls of White and Scalapino [27]. This phase is stable up to $V \simeq 1.0$.

At larger $V > 1.0$ the ground state changes and one finds first the nine-site islands of an AF phase separated by nonmagnetic domain walls in both directions, with the alternating larger/smaller charge densities along the walls. At $V \simeq 1.3$ the vertical stripes are stable again, but the lines which separate them are FM and have a pronounced charge alternation along them. Note that the experimental data of Tranquada *et al* [2] were first interpreted assuming such an alternation of charge densities. Starting from $V = 1.5$, imperfect CO phases are the most stable ones. The charges roughly resemble a bipartite lattice, however with sizable charge inhomogeneities. This phase (see figure 4) consists of domains of quite imperfect CO phase with AF order (somewhat similar to a stripe) and the classical nonmagnetic CO domains (with an almost empty charge-minority sublattice).

For larger doping ($\delta = 1/4$), one finds vertical stripes for $0.0 < V < 1.0$, and for $V = 1.35$ to 1.5. Surprisingly, between $V = 1.05$ and 1.20 the diagonal stripes are more stable (left-hand panel, figure 5). This latter phase has nonmagnetic diagonal domain walls, similar to those found at $U = 4$ and $V < 0.3$ for $\delta = 1/8$. This result demonstrates that the intersite Coulomb interaction can *induce* the stripe order at larger doping, where the tendency towards separation into the charge-poor and charge-rich regimes is enhanced. However, large values of V destroy the stripe order also in this case (as for $\delta = 1/8$), and one finds the slightly inhomogeneous bipartite lattice CO phase with a superimposed spin order in the entire interval from $V = 1.65$ to 3.0 (figure 5).

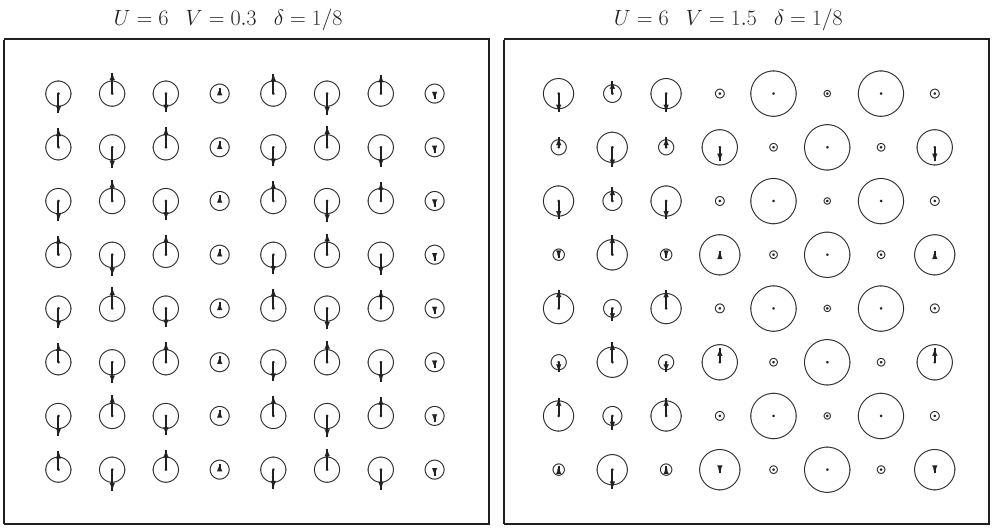

Figure 4. Magnetic and charge order as obtained for an 8×8 cluster with $U = 6$ and $V = 0.3$ (left) and $V = 1.5$ (right) at doping $\delta = 1/8$. The meaning of circles and arrows is the same as in figure 2.

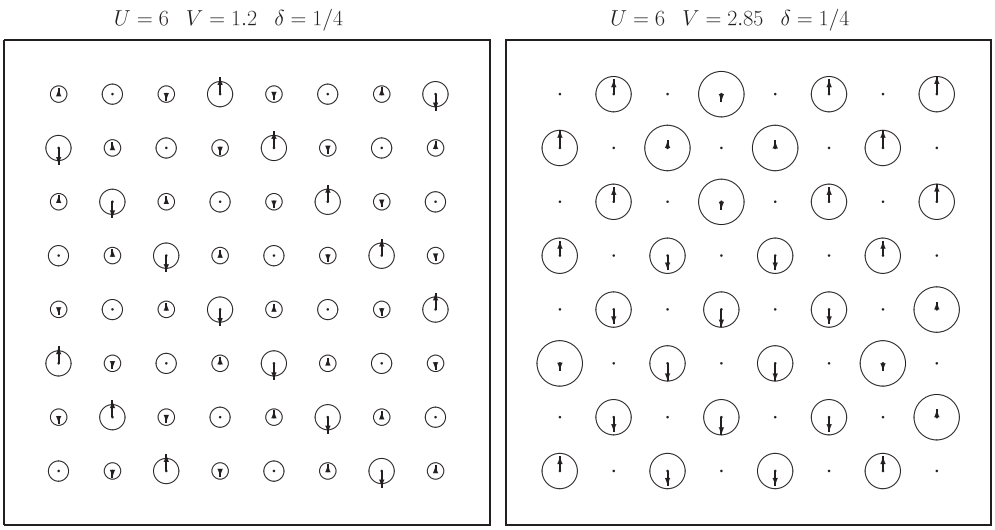

Figure 5. Magnetic and charge order as obtained for an 8×8 cluster with $U = 6$ for $V = 1.2$ (left) and $V = 2.85$ (right) at doping $\delta = 1/4$. The meaning of circles and arrows is the same as in figure 2.

For the case of quarter filling ($\delta = 1/2$) the charge is invariably ordered in a highly symmetric way which could be termed a superstripe, or better a superlattice-type ordering (not shown). For small $V < 1.5$ polaronic islands with small magnetic moments were found, while the CO dominates at large values of V. Starting from $V = 1.8$ up to 3.0 one finds the ideal bipartite lattice CO with one (almost) empty sublattice, exactly the same as shown in the right-hand panel of figure 3.

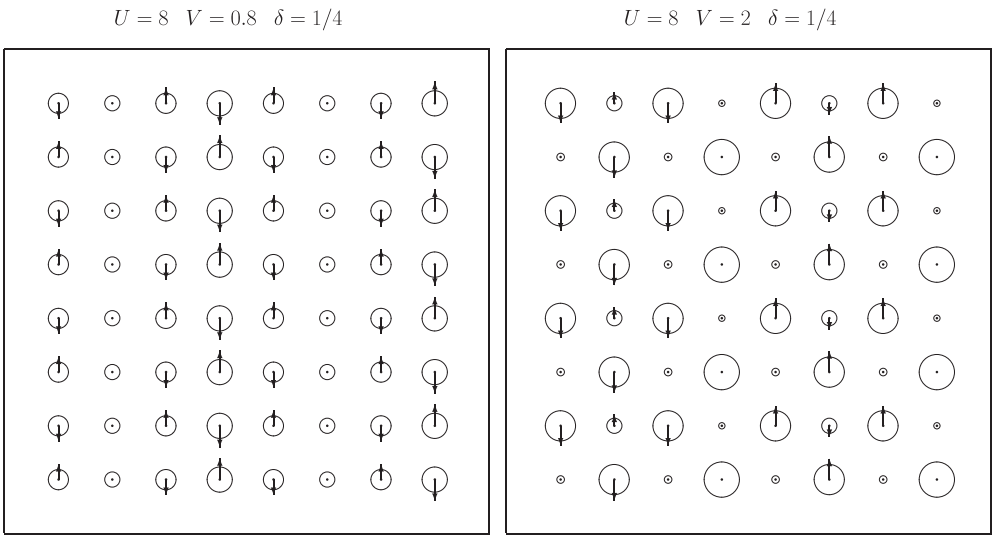

Figure 6. Crossover from stripe phase (left) to CO (right) as obtained for an 8×8 cluster with $U = 8$ at doping $\delta = 1/4$. The panels show the stable structures found for $V = 0.8$ and 2.0. The meaning of circles and arrows is the same as in figure 2.

4.4. Charge order in the strong coupling regime, $U \geqslant 8$

The stable phases at $U = 8$ and $\delta = 1/8$ are quite similar to those reported above for $U = 6$ and $\delta = 1/8$, i.e., one finds various stripe phases in the regime of low intersite Coulomb repulsion $0 \leqslant V \leqslant 1.8$. The imperfect CO phase with magnetic and nonmagnetic domains sets in for $V > 1.8$ (a similar one to that shown in figure 4).

At larger doping ($\delta = 1/4$) the stripe order is even more robust. The vertical nonmagnetic stripe walls here separate AF domains, consisting of three atoms along the direction perpendicular to the walls, in the entire range $0 \leqslant V \leqslant 1.8$ (see the left-hand panel of figure 6). This demonstrates once again that finite V stabilizes stripe phases in the large doping regime. For $V > 1.8$, the imperfect CO coexists with an imperfect spin order (see the right-hand panel of figure 6).

For quarter filling ($\delta = 1/2$) the situation is again similar to that found for $U = 6$. Highly symmetric charge patterns of superlattice type are the most stable ones for $V < 1.2$ (not shown). On the one hand, such patterns, having unit cells increased by a factor of two, can be called superlattice (or superstripes), but on the other hand, they can be seen as precursor charge patterns to the CO phase. In fact, CO with a small amplitude of charge variation between majority and minority sublattices is already visible in this case. An interesting finding in this regime is the sporadic appearance of local hexagonal patterns. The ideal CO phase (see the right-hand panel of figure 3), with coexisting AF order at the charge-majority sublattice, starts from $V \simeq 1.2$.

For Coulomb interaction increased up to $U = 10$, one finds a similar evolution of the ground state on changing V as for the $U = 8$ case. At low doping ($\delta = 1/8$), first various stripe phases are stable in the interval between $V = 0.0$ and 2.5 (some of them look identical to those found for $U = 8$, while others are only quantitatively different). Next, for $V > 2.5$ the imperfect CO phases with coexisting nonmagnetic and magnetic regions are the most stable phases. The typical pattern is similar to that found already at $U = 8$ and shown in the right-hand panel of figure 6.

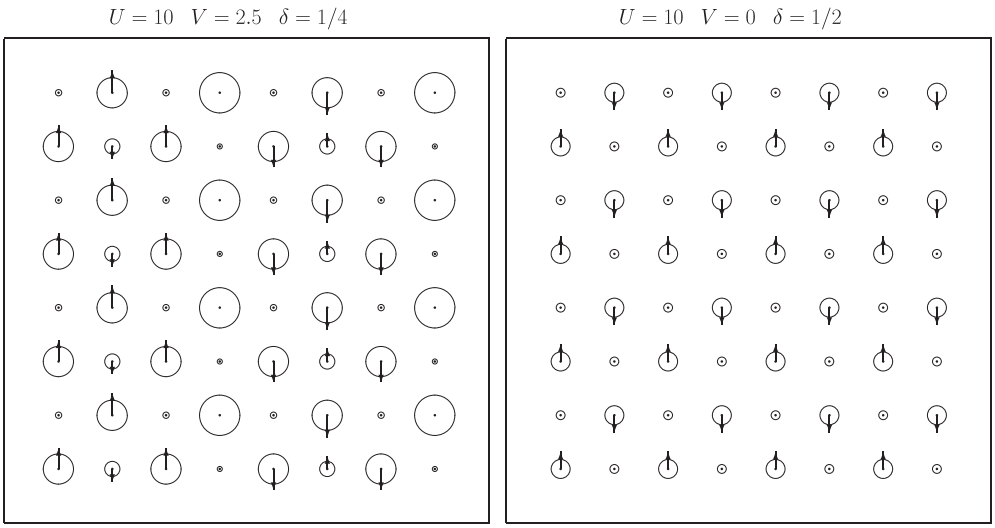

Figure 7. Coexisting magnetic and charge order as obtained for an 8×8 cluster with $U = 10$, and $V = 2.5$, $\delta = 1/4$ (left) and $V = 0$, $\delta = 1/2$ (right). The meaning of circles and arrows is the same as in figure 2.

The stripe phase found at doping $\delta = 1/4$, stable in between $V = 0.0$ and 2.25 at $U = 10$, has quite different charge densities at neighbouring sites, and might be therefore called an imperfect CO phase as well. The CO takes over starting from $V = 2.5$, and coexists with the imperfect magnetic order (left-hand panel of figure 7). This phase can be viewed as a superposition of the CO and magnetic domains, separated by the nonmagnetic domain walls with CO along them. The CO is here superimposed on the magnetic structure, and thus the magnetic moments on the atoms with large charge density are amplified. As a result, the magnetic domains which were AF in the stripe phases for $V < 2.5$ have net FM moment and a weak AF component at the sublattice with low charge density.

At quarter filling ($\delta = 1/2$) and large $U = 10$, the two-sublattice CO phase is induced for all $V \geqslant 0$ (see the right-hand panel of figure 7). The CO coexists here with the AF order on the charge-majority sublattice. By comparing this phase with virtually the same charge and magnetization density distribution shown in the right-hand panel of figure 3, we conclude that a generic tendency towards the CO phase is present at doping $\delta = 1/2$ in the strong coupling regime, while finite V is required to stabilize this phase in the weak coupling regime of $U \simeq 4$.

5. Discussion and conclusions

5.1. Robust versus method-dependent results

We would like to emphasize that our study has a qualitative character, and some of the results presented can turn out to be 'method- and/or cluster-dependent' ones. However, we are confident that such features as (i) the appearance of stripe phases for small V and weak doping, and (ii) the crossover to the CO phases with the coexisting magnetic patterns found for larger V, and (iii) enhanced tendency towards stripe order at doping $\delta = 1/4$ when V is finite are robust.

The change to larger clusters, or the change of the computational scheme, would not influence them. But of course, such details as the precise distribution of charge density, charge and spin patterns within the stripe phases, belong to second category; that is, they are difficult to determine and could be to some extent modified when the computational method is improved.

By comparing different possible choices of local operators one can conclude that the correlation method employed captures the essential part of the electronic correlations. We have verified that the generalized Gutzwiller method employing only one type of the local operators, $\delta n_{i\uparrow}\delta n_{i\downarrow}$, gives inferior results with respect to our LI + LA method with all three types of local operators. However, we do not expect that including more local operators would improve the correlation energy in a significant way.

5.2. Summary and conclusions

One of the most important features of the present investigation is the multitude of possible ground states occurring for various U and V and for different doping and the multitude of metastable states, with their energies being sometimes quite close to the ground states. Although no simple, transparent and easy to classify physical picture emerges, we believe that the observed behaviour is generic for doped systems with medium to strong intrasite and intersite Coulomb interactions. In other words, the predictions of the exact ground state symmetry and charge and spin patterns is a difficult task.

In section 4 we discussed in a systematic manner the order of appearance of stripe, CO and mixed phases when one varies the control parameters, i.e., the doping, the intersite V and the intrasite U Coulomb interactions. Although there are some underlying organizing principles, the picture is far from simple. However, we have seen that large Coulomb interactions promote inhomogeneous charge distribution *even without* any coupling to the lattice or disorder effects [28]. There, we conclude that the tendency towards inhomogeneous charge distribution is generic in doped systems. Indeed, such inhomogeneous charge patters characterize dynamical stripes in the cuprates, as shown recently in the framework of the spin-fermion model [29].

Nevertheless, on top of this complexity some simple rules do exist, good enough to make certain qualitative predictions. We have found that the stripe structures are typical for small doping ($\delta = 1/8$), and rather small intersite repulsion V, while for larger V CO phases appear instead. The second rule is that at larger dopings CO ground states are favoured. The case of quarter filling ($\delta = 1/2$) is particular: here the CO is easily stabilized, and the magnetic order occurs at the sublattice with larger charge density. Such states play an important role in the half-doped manganites.

As a closing remark let us recall once more that we studied the stable structures only at $T = 0$. While the CO disappears at sufficiently high temperature, at some intermediate value T another phase transition might occur—from the ideal CO phase to some other phase with a different CO pattern (or to a stripe phase, or even to a more complex mixed phase), as recently found in the nickelates [11]. Thus, the CO detected experimentally at finite T might not necessarily be the same one as that found at $T = 0$.

Acknowledgment

We acknowledge the financial support by the Polish State Committee of Scientific Research (KBN), Project No. 5 P03B 036 21.

References

[1] Zaanen J and Gunnarsson O 1989 *Phys. Rev.* B **40** 7391
[2] Tranquada J M, Sternlieb B J, Axe J D, Nakamura Y and Uchida S 1995 *Nature* **375** 561
Tranquada J M, Axe D J, Ichikawa N, Nakamura Y, Uchida S and Nachumi B 1996 *Phys. Rev.* B **54** 7489

Tranquada J M, Axe J D, Ichikawa N, Moodenbaugh A R, Nakamura Y and Uchida S 1997 *Phys. Rev. Lett.* **78** 338
Yamada K, Lee C H, Endoh Y, Shirane G, Birgeneau R J and Kastner M A 1997 *Physica* C **282–287** 85
Wakimoto S, Shirane G, Endoh Y, Hirota K I, Ueki S, Yamada Y, Birgenau R J, Kastner M A, Lee Y S, Gehring M P and Lee S H 1999 *Phys. Rev.* B **60** 769
Wakimoto S, Birgenau R J, Kastner M A, Lee Y S, Erwin R, Gehring P M, Lee S H, Fijuta M, Yamada K, Endoh Y, Hirota K and Shirane G 2000 *Phys. Rev.* B **61** 3699
[3] Tranquada J M, Buttrey D J, Sachan V and Lorenzo J E 1994 *Phys. Rev. Lett.* **73** 1003
Sachan V, Buttrey D J, Tranquada J M and Lorenzo J E 1995 *Phys. Rev.* B **51** 12742
Tranquada J M, Lorenzo J E, Buttrey D J and Sachan V 1995 *Phys. Rev.* B **52** 3581
[4] Zaanen J and Littlewood S 1994 *Phys. Rev.* B **50** 7222
Mizokawa T and Fujimori A 1997 *Phys. Rev.* B **56** 11920
[5] Seibold G, Castellani C, Di Castro C and Grilli M 1998 *Phys. Rev.* B **58** 13506
[6] Ohiani A, Suzuki T and Kasuya T 1990 *J. Phys. Soc. Japan* **59** 4129
[7] Ohama T, Yasuoka H, Isobe M and Ueda Y 1999 *Phys. Rev.* B **59** 3299
[8] Wollan E O and Koeller W C 1955 *Phys. Rev.* **100** 545
Tomioka Y, Asimitsu A, Moritomo Y, Kawahara H and Tokura Y 1995 *Phys. Rev. Lett.* **74** 5108
Chen C H and Cheong S W 1996 *Phys. Rev. Lett.* **76** 4042
Kawano H, Kajimoto R, Yoshizawa H, Tomioka Y, Kuwahara H and Tokura Y 1997 *Phys. Rev. Lett.* **78** 4253
Kubota M, Yoshizawa H, Moritomo Y, Fujioka H, Hirota K and Endoh Y 1999 *J. Phys. Soc. Japan* **68** 2202
[9] Ishikawa T, Ookura K and Tokura Y 1999 *Phys. Rev.* B **59** 8367
Argyriou D N, Bordallo H N, Campbell B J, Cheetham A K, Cox D E, Gardner J S, dos Santos A and Strouse G F 2000 *Phys. Rev.* B **61** 15269
[10] Sternlieb B J, Hill J P, Wildgruber U C, Luke G M, Nachumi B, Moritomo Y and Tokura Y 1996 *Phys. Rev. Lett.* **76** 2169
Murakami Y, Kawada H, Kawata H, Tanaka M, Arima T, Moritomo Y and Tokura Y 1998 *Phys. Rev. Lett.* **80** 1932
[11] Kajimoto R, Ishizaka K, Yoshizawa H and Tokura Y 2003 *Phys. Rev.* B **67** 014511
Yamamoto K, Ishizaka K, Saitoh E, Shinomori S, Tanabe T and Katsufui T 2003 *Phys. Rev.* B **67** 014414
[12] Robaszkiewicz S 1974 *Acta Phys. Pol.* A **45** 289
[13] Oleś A M, Micnas R, Robaszkiewicz S and Chao K A 1984 *Phys. Lett.* A **102** 323
[14] Hirsch J E 1984 *Phys. Rev. Lett.* **53** 2327
[15] Seo H and Fukuyama H 1998 *J. Phys. Soc. Japan* **67** 2602
[16] van Dongen P G J 1994 *Phys. Rev.* B **50** 14016
van Dongen P G J 1994 *Phys. Rev.* B **54** 1584
[17] Pietig R, Bulla T and Blawid S 1999 *Phys. Rev. Lett.* **82** 4046
[18] Hellberg C S 2001 *J. Appl. Phys.* **89** 6627
[19] Vojta M 2002 *Phys. Rev.* B **66** 104505
[20] Hoang A T and Thalmeier P 2002 *J. Phys.: Condens. Matter* **14** 6639
[21] Stollhoff G and Fulde P 1980 *J. Chem. Phys.* **73** 4548
Stollhoff G 1996 *J. Chem. Phys.* **105** 227
Fulde P 1991 *Electron Correlations in Molecules and Solids* (*Springer Series in Solid State Sciences* vol 100) (Berlin: Springer)
[22] Góra D, Rościszewski K and Oleś A M 1999 *Phys. Rev.* B **60** 7429
[23] Stoll H 1992 *Phys. Rev.* B **46** 6700
Stoll H 1992 *Chem. Phys. Lett.* **181** 548
Stoll H 1992 *J. Chem. Phys.* **97** 8449
Stoll H 1996 *Ann. Phys., Lpz* **5** 355
[24] Paulus B, Fulde P and Stoll H 1995 *Phys. Rev.* B **51** 10572
Doll K, Dolg M, Fulde P and Stoll H 1995 *Phys. Rev.* B **52** 4842
Paulus B, Fulde P and Stoll H 1996 *Phys. Rev.* B **54** 2556
Doll K, Dolg M and Stoll H 1996 *Phys. Rev.* B **54** 13529
Kalvoda S, Paulus B, Fulde P and Stoll H 1997 *Phys. Rev.* B **55** 4027
Paulus B, Shi F-J and Stoll H 1997 *J. Phys.: Condens. Matter* **9** 2745
Doll K, Dolg M, Fulde P and Stoll H 1997 *Phys. Rev.* B **55** 10282
Yu M, Kalvoda S and Dolg M 1997 *Chem. Phys.* **224** 121
Kalvoda S, Dolg M, Flad H, Fulde P and Stoll H 1998 *Phys. Rev.* B **57** 2127
Shukla A, Dolg M, Fulde P and Stoll H 1999 *Phys. Rev.* B **60** 5211

Rościszewski K, Paulus B, Fulde P and Stoll H 1999 *Phys. Rev.* B **60** 7905
Rościszewski K, Paulus B, Fulde P and Stoll H 1999 *Phys. Rev.* B **62** 5482
Albrecht M, Fulde P and Stoll H 2000 *Chem. Phys. Lett.* **398** 355
[25] Kopka H and Daly W P 1999 *A Guide to LaTex* (New York: Addison-Wesley)
[26] Fleck M, Lichtenstein A I, Pavarini E and Oleś A M 2000 *Phys. Rev. Lett.* **84** 4962
[27] White S R and Scalapino D J 1998 *Phys. Rev. Lett.* **80** 1272
[28] Burgy J, Mayr M, Martin-Mayor V, Moreo A and Dagotto E 2001 *Phys. Rev. Lett.* **87** 277202
[29] Moraghebi M, Yunoki S and Moreo A 2002 *Phys. Rev. Lett.* **88** 187001